Chapter V:
Stellar structure and evolution of single stars

https://doi.org/10.1017/S1743921322003349 Published online by Cambridge University Press

Massive Stars Near and Far
Proceedings IAU Symposium No. 361, 2024
J. Mackey, J. S. Vink, & N. St-Louis, eds.
doi:10.1017/S1743921322003349

Stellar Structure and Evolution of Massive Rotating Single Stars

R. Hirschi[1,2], E. Kaiser[1], P. Eggenberger[3], S. Ekström[3], C. Georgy[3], A. Maeder[3] and G. Meynet[3]

[1]Astrophysics Group, Lennard-Jones Laboratories, Keele University, Keele ST5 5BG, UK
email: r.hirschi@keele.ac.uk

[2]Kavli IPMU (WPI), University of Tokyo, 5-1-5 Kashiwanoha, Kashiwa 277-8583, Japan

[3]Geneva Observatory, Geneva University, CH-1290 Sauverny, Switzerland

Abstract. Rotation plays an important role in the structure and evolution of massive stars. It leads to deviation from spherical symmetry for very fast rotating stars, mixing in otherwise unmixed radiative regions and generally increased mass loss. In addition, magnetic fields interact with rotation and lead to significant transport of angular momentum. In this article, we review the various rotational and magnetic instabilities present in massive stars and their implementation in one-dimensional stellar evolution codes. We then focus on their impact on the evolution of single rotating stars. Finally, we compare rotating models to observations and discuss ways to disentangle between various uncertainties.

Keywords. rotation - hydrodynamics - magnetism - stars: evolution, interiors, massive

1. Structure and Evolution Models of Rotating Stars

Modelling the evolution of stars and populations of stars is still generally limited to one-dimensional (1D) models though the number and range of multi-dimensional hydrodynamic simulations are growing as demonstrated by many contributions in these proceedings (see e.g. contributions by Rieutord and Rizzuti in this Session). 1D models make the assumption of spherical symmetry, which means that physical quantities such as temperature and pressure are considered to be constant on spherical shells and only depend on radius. The mass enclosed by a shell is usually preferred to the radius as the independent variable in the Lagrangian description used in stellar models. The structure of a star can then be obtained by solving the 1D version of the four stellar structure equations (conservation of mass, momentum and energy as well as energy transfer). Modelling the evolution of stars requires additional physics and equations related to nuclear reactions, mass loss, convection, rotation, magnetic fields, binary interactions, equation of state, opacities, neutrino losses, etc. including their dependence on metallicity.

We will focus here on rotation and magnetic fields and their interactions (see other contributions for the other aspects). Rotation has several effects on the structure and evolution of stars. Axial rotation opposes the effects of gravity (centrifugal force) and thus breaks spherical symmetry. It is, however, possible to keep stellar structure equations 1D (sometimes referred to as 1.5D) by making the assumption of shellular rotation (Zahn 1992). This assumes that instabilities can act much faster perpendicular to gravity (i. e. strong horizontal turbulence on isobars) and leads to constant angular velocity on isobars. Other quantities like density and temperature are not constant on isobars and averages must be used in the structure equations (see Meynet & Maeder 1997, for more details). Angular velocity and angular momentum generally vary across the star (unless solid body

rotation is imposed, which is usually done at the start of the evolution or in convective regions). The evolution of rotation is modelled using the additional equation of angular momentum transport (the conserved quantity). Other key effects of rotation include enhanced mass loss (see Langer 1998; Maeder & Meynet 2000; Gagnier et al. 2019a, for details and discussions) and internal transport of angular momentum and mixing of the chemical composition in otherwise unmixed radiative zones. Magnetic fields bring further deviations from spherical symmetry and a rotating magnetic star would ideally be modelled using 3D magneto-hydrodynamic simulations (see e.g. Braithwaite & Spruit 2004; Varma & Müller 2021; Yoshida et al. 2021). To simulate the long-term evolution of stars, however, 1D theoretical prescriptions have to be used to model the evolution of magnetic fields and their interactions with rotation.

2. Internal Transport Mechanisms

There are many internal transport mechanisms at play in massive stars: convection, internal gravity waves (e.g. Talon & Charbonnel 2005; Edelmann et al. 2019), rotational (aka hydrodynamic) and magnetic instabilities. Note that in binary stars, tidal effects (Section 4; e. g. Zahn 1977; Ogilvie 2014), are also able to redistribute angular momentum and composition. We limit here the discussion to rotational and magnetic instabilities.

2.1. *Rotational Instabilities*

The two dominant rotational instabilities are meridional (aka Eddington-Sweet) circulation (Talon & Zahn 1997; Zahn 1992; Maeder & Zahn 1998; Maeder 2009) and shear instabilities. Other instabilities have been identified: Solberg-Hoiland, GSF, etc. but they are unlikely to significantly change the evolution of stars (Heger et al. 2000; Hirschi et al. 2004; Caleo et al. 2016). Meridional circulation is driven by the thermal gradients on isobars (polar regions have higher gravity and radiative fluxes and thus are hotter than the equatorial regions). The circulation can transport angular momentum both inward and outward and thus can both build and reduce angular velocity gradients depending on the direction of the circulation (see fig. 1 in Meynet & Maeder 2002). Indeed, angular momentum is transported inward when the circulation goes outward at the pole (where the angular momentum is zero) and inward at the equator and vice versa. Shear instabilities develop when there is differential rotation inside the star since, in this case, adjacent layers move laterally with respect to each other and experience a strain. Shear instabilities can take place on dynamical timescales if the excess kinetic energy is larger than the work against the buoyancy force needed to overturn the shear layer. Dynamical shear is fast but generally limited to very narrow regions at the edge of convective regions and it thus has a very small impact on the structure and evolution of rotating stars (Hirschi et al. 2004; Hirschi & Maeder 2010; Edelmann et al. 2017). When the shear layers are dynamically stable, thermal diffusion can help shear transport angular momentum and composition on a much longer, secular timescale (Zahn 1974; Maeder 1997). Shear, whether dynamical or secular, mixes regions together so can only reduce gradients.

Shear mixing obviously only takes place when there is a gradient of angular velocity. It is important to note that this is not the case with meridional circulation, which can occur even when the star has solid body rotation. Circulation instead will be quite sensitive to the assumptions made concerning the horizontal turbulence. As the evolution proceeds, chemical composition (μ) gradients develop, which will inhibit both instabilities (see Frischknecht et al. 2010, for how the evolution on the MS affects these instabilities).

2.2. *Magnetic Instabilities*

Various magnetic instabilities have been studied in the context of massive stars. Here we will only discuss the Tayler-Spruit dynamo (Spruit 2002; Heger et al. 2005) and its

https://doi.org/10.1017/S1743921322003349 Published online by Cambridge University Press

modification by Fuller et al. (2019). Other instabilities include the magneto-rotational instabilitiy (Wheeler et al. 2015; Griffiths et al. 2022) and the $\alpha - \Omega$ dynamo (Potter et al. 2012b). For fossil fields and the connection between magnetic fields and mass loss, see Session 3 (physical processes). In the Tayler-Spruit dynamo (TS dynamo hereinafter; see Tayler 1973; Spruit 2002; Heger et al. 2005; Maeder & Meynet 2005, for details), an initially very small seed field is assumed. Due to differential rotation, the radial component (B_r) of the field is wound up and the azimuthal component (B_ϕ) is thus amplified. The Tayler (pinch-type) instability then generates a stronger radial component (B_r), thus closing the amplification loop. The amplification saturates at the point where the amplification and damping (dominated by magnetic diffusivity) timescales become equal. A minimum amount of differential rotation (denoted $q_{\rm min}$) is required to trigger this instability meaning that the instability is not present in the case of solid body rotation.

Fuller et al. (2019) propose modifications to the Tayler-Spruit dynamo (FTS dynamo hereinafter). The main ones are the component of the magnetic fields (background versus perturbed component) being wound up (perturbed radial field in Spruit 2002) and damped (background azimuthal field damped in Spruit 2002). Both these changes lead to higher saturation levels of the magnetic fields and enhanced transport.

2.3. *Implementation in 1D Stellar Evolution Codes*

Magnetic instabilities (both TS and FTS dynamos) like shear instabilities lead to transport of angular momentum and chemical composition that is suitably represented as a diffusive process (using an effective diffusion). As written above, meridional circulation, on the other hand, can both build and reduce gradients of angular momentum and is thus best described with an advective term in the angular momentum transport equation as done in `GENEC` (Eggenberger et al. 2008; Ekström et al. 2012) and several other codes `FRANEC` (Chieffi & Limongi 2013) and `STARS/ROSE` (Potter et al. 2012a). Taking into account an advective term, however, leads to a fourth-degree equation that is time consuming and difficult to solve. Several other codes `MESA` (e.g. Paxton et al. 2013) `STERN` and `KEPLER` (e.g. Heger et al. 2000; Petrovic et al. 2005), thus treat the meridional (Eddington-Sweet) circulation as a diffusive process. For the transport of chemical elements, all the above instabilities lead to mixing that can be treated as diffusion and for which an effective diffusion coefficient is used for the combined effect of meridional circulation and horizontal turbulence in `GENEC`. In addition to whether meridional circulation is treated as an advective or diffusive process, there are further differences in between codes in the formulae used for specific instabilities as well as parameters modifying the strength of these (e.g. f_c and f_μ, see Heger et al. 2000, for details), which are calibrated to sets of observations. One thus has to be careful when comparing rotating models calculated with different codes, even when they include the same physical processes.

3. Structure and Evolution of Massive Rotating Stars

Massive stars go through six burning phases (H, He, C, Ne, O and Si) after which their iron core collapses into a neutron star or black hole. The evolution of the structure of as star can be summarised in the structure evolution diagram (aka Kippenhahn diagram), an example of which is presented in Fig. 1 for a $15\,{\rm M}_\odot$ non-rotating model. This figure includes iso-radius contour lines ($\log_{10}(r)$). These nicely show how the core of massive stars contracts (contours moving up in mass coordinate) throughout their evolution. Contraction is modest during a burning stage but then accelerates at the end of each burning phase when nuclear reactions no longer counteracts the gravitational force. The contraction stops (and is sometimes even slightly reversed) when a high enough temperature is reached in the core for the next burning phase to start. The envelope of massive

https://doi.org/10.1017/S1743921322003349 Published online by Cambridge University Press

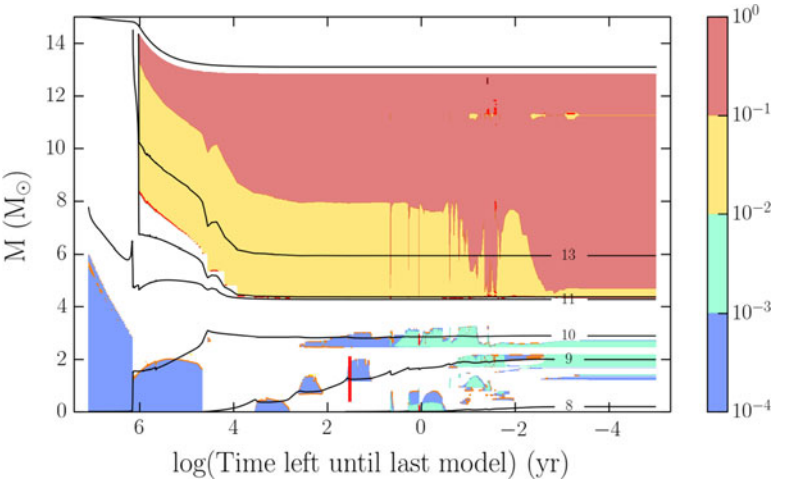

Figure 1. Structure evolution diagram of the 15 $M_\odot$ (non-rotating) solar metallicity GENEC stellar model. The horizontal axis is a logarithmic scale of the time left before the predicted collapse of the star in years (the last model in this simulation is before the end of silicon burning but since the time-scale of silicon burning is so short this does not affect the plot for the earlier phases) and the vertical axis is the mass coordinate in solar masses. The total mass and radial contours (in the form $\log_{10}$(r) in cm), are drawn as solid black lines. Shaded areas correspond to convective regions. The colour indicates the value of the Mach number (figure taken from Cristini et al. 2017).

stars, on the other hand, expands through most of their evolution with the largest and fastest expansion taking place at the end of the main sequence (MS) when most massive stars become red or blue supergiants (WR stars do not expand as much). Key effects of rotation on the structure and evolution of massive stars are enhanced mass loss and larger core masses (due to mixing in radiative zones) leading to rotating stars evolving like more massive non-rotating stars (see e. g. Hirschi et al. 2004, for details).

3.1. *Evolution of Rotation*

The evolution of rotation inside a massive stars is predominantly driven by the core contraction and envelope expansion described above and by convective regions (coloured regions in Fig 1) efficiently redistributing angular momentum within these regions. Given that angular momentum is conserved and that the specific angular momentum, j, is proportional to Ωr^2, a contraction (expansion) leads to an increase (decrease) in the angular velocity (Ω). This explains why the angular velocity (Ω) increases in the core and generally decreases in the envelope throughout the evolution. Fig. 2 (*left*) shows the evolution of the angular velocity for a GENEC 25 $M_\odot$ rotating stellar model. This model loses its H-rich envelope during He-burning and thus loses its very low Ω tail by C-burning. Stellar evolution models assume that convective regions rotate as solid bodies so have a flat angular velocity profile (though see question at the end). This explains the flat Ω profiles in the core during various burning phases and in the convective envelope (see left panels in Fig. 3). By the end of the evolution, Ω reaches values around 1 s^{-1}.

To determine if angular momentum is transported between the core and envelope or lost by stellar winds, it is easier to consider the evolution of the specific angular momentum (j) profiles (see Fig. 2 *right* panel), which are not modified by contraction or expansion. In GENEC models, meridional circulation and shear transport j out of the core mostly during H-burning and to a smaller extent during core He-burning. During the advanced phases, only convection has the time to redistribute angular momentum, creating a saw-tooth

https://doi.org/10.1017/S1743921322003349 Published online by Cambridge University Press

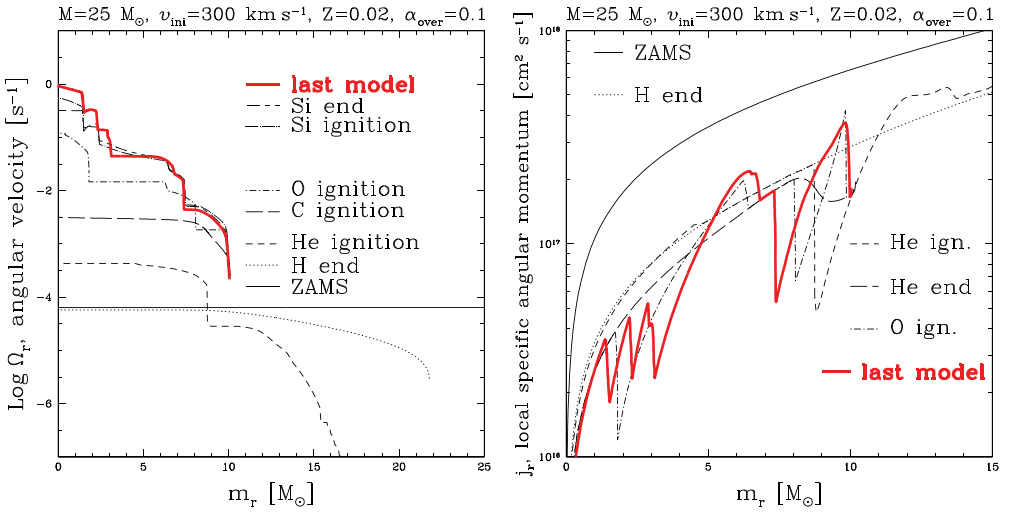

Figure 2. Angular velocity (*Left*) and local specific angular momentum profiles as a function of the Lagrangian mass coordinate, m_r, inside the 25 $M_\odot$ model ($v_{\rm ini} = 300$ km s^{-1}) `GENEC` solar metallicity model at various evolutionary stages (figure taken from Hirschi et al. 2004).

pattern given the assumption of constant Ω in convective regions. Mass loss removes a significant amount of mass, more than half the initial mass in this 25 $M_\odot$ model. This demonstrates the crucial effect of mass loss for stars above $25 - 30\,M_\odot$. Angular momentum being highest at the surface, stellar winds also remove significant amount of angular momentum from massive stars. Rotation in the core, however, is more affected by internal transport than mass loss at the surface as discussed below.

Before discussing magnetic instabilities, it is instructive to compare non-magnetic rotating models since, as discussed above, different theoretical prescriptions are used in different codes and their technical implementation differ too. The discussion here is limited to one representative `GENEC` model (Fig. 2) taken from Hirschi et al. (2004) (see Frischknecht et al. 2010; Ekström et al. 2012; Chieffi & Limongi 2013, for more detailed discussions) and one representative `MESA` model (*top* row of Fig. 3) taken from Kaiser (2021, see Sect. 2.3 for references to other similar codes). The surface rotation is different because the 25 $M_\odot$ (`GENEC`) model loses its H-rich envelope while the 15 $M_\odot$ (`MESA`) model does not. This is explained by mass loss. The core angular velocity (*left* panels), at first sight, appear to evolve in a similar way with the increase in Ω explained by the contraction of the core. There are key differences, however, in the timing and extent of the angular momentum transport (*right* panels) between the core and envelope. The first one is the absence of j transport between the core and envelope during the MS in the `MESA` model. The second is the smaller overall decrease in the specific angular momentum. These are mainly due to breaks in the transport just above convective cores where composition gradients inhibit instabilities (see Kaiser 2021, for a detailed discussion). Despite these differences, we see that both these `GENEC` and `MESA` non-magnetic models end with a core angular velocity, $\Omega \sim 1\,{\rm s}^{-1}$.

4. Magnetic Instabilities and their Effect on Internal Rotation

Values of $\Omega \sim 1\,{\rm s}^{-1}$ at the end of the evolution of massive stars are too high to explain the observed rotation rate of pulsars (see comparison below). Such models would actually predict neutron stars at critical rotation and this discrepancy between models and observations is one of the main drivers to include magnetic instabilities in stellar models

https://doi.org/10.1017/S1743921322003349 Published online by Cambridge University Press

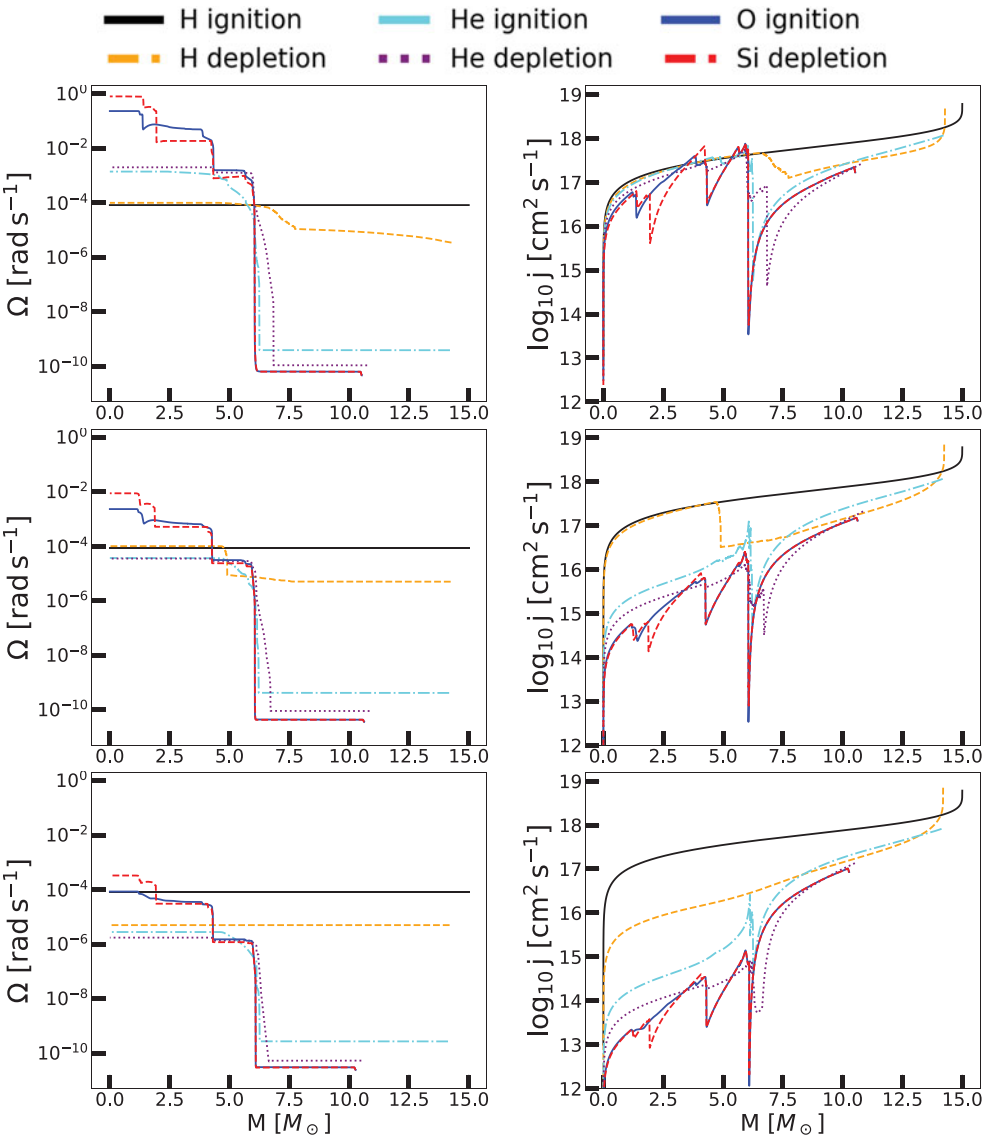

Figure 3. Evolution of rotation profiles for 15 $M_\odot$ `MESA` models including different angular momentum transport mechanisms, *top*: without magnetic fields, *middle*: TS dynamo, *bottom*: FTS dynamo, showing on the left panel the angular rotation velocity, Ω, and on the right panel the specific angular momentum, j. Each line presents the profile at a different evolutionary stage indicated by the colour and linestyle (see legend on top). To enable a better comparison, the axis of each thematic subplot group has been scaled to the same values. These models were computed with the `MESA` stellar evolution code (Paxton et al. 2011, 2013, 2015, 2018), revision 10108 (figure adapted from multiple figures from Kaiser 2021).

to solve this issue (e.g. Heger et al. 2000, 2005; Petrovic et al. 2005; Hirschi et al. 2005; Wheeler et al. 2015; Ma & Fuller 2019).

4.1. *Taylor-Spruit and Fuller-modified Taylor-Spruit Dynamos*

We briefly investigate here the impact of the TS or FTS dynamos on the evolution of rotation in 15 $M_\odot$ `MESA` models (with an initial rotation corresponding to $\Omega/\Omega_{\rm crit} = 0.4$)

https://doi.org/10.1017/S1743921322003349 Published online by Cambridge University Press

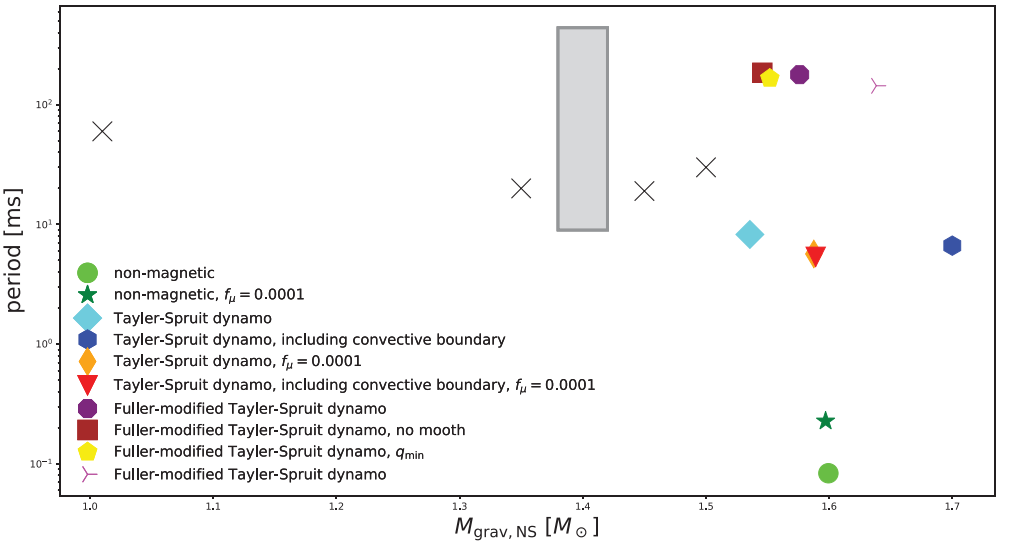

Figure 4. Observed (black crosses) and predicted (coloured symbols) neutron star spin period as a function of the gravitational mass for various $15\,M_\odot$ models including the ones from Fig. 3. The black crosses show observed neutron star spins by Muslimov & Page (1996) and Faucher-Giguère & Kaspi (2006). The grey rectangle depicts an observed range of neutron star spins (Marshall et al. 1998; Kaspi & Helfand 2002; Faucher-Giguère & Kaspi 2006; Popov et al. 2010; Popov & Turolla 2012; Gotthelf et al. 2013) with an assumed neutron star mass of $1.4\,M_\odot$ (figure taken from Kaiser 2021).

and compare these models to a non-magnetic model in Fig. 3. Even though it has a limited impact during the MS (see discussion in Kaiser 2021), the magnetic dynamo viscosity in the TS dynamo model (*middle* panels) is much stronger than the rotational instabilities included in the non-magnetic model (*top* panels). This leads to a strong transport of angular momentum out of the core between the end of core H-burning and the start of core He-burning (the period of strong core contraction and envelope expansion) and a much reduced final angular velocity profile, $\Omega \sim 10^{-2}\,\mathrm{s}^{-1}$. Considering now the FTS dynamo model (*bottom* panels), the even larger magnetic dynamo viscosity already operates during the MS and leads to an even lower core angular velocity, $\Omega \sim 10^{-4}\,\mathrm{s}^{-1}$.

4.2. *Predicted Rotation Rate of Pulsars*

Figure 4 presents the predicted estimated neutron star period as a function of the gravitation mass, $M_{\mathrm{grav,NS}}$, for $15\,M_\odot$ models at solar metallicity with different angular momentum transport assumptions (see legend for key assumptions). The spin period and the gravitational mass are computed following Heger et al. (2005), their Section 3.4. Additionally, Fig. 4 also includes observed spin periods of young neutron stars. A few neutron stars have fast natal spin periods of 11 ms (Marshall et al. 1998) or 20 ms (Muslimov & Page 1996; Kaspi & Helfand 2002) but the majority rotate slower with a spin period of $50 - 100$ ms (Muslimov & Page 1996; Faucher-Giguère & Kaspi 2006; Popov et al. 2010; Popov & Turolla 2012). There are also a few very slowly rotating neutron stars with a natal spin of up to 400 ms (Gotthelf et al. 2013). The comparison between the model predictions and observations reveals several points. First, the three different angular momentum transport combinations predict three distinct ranges for the spin period of neutron stars, independently of the various related uncertainties in angular momentum transport (e.g. spatial and temporal smoothing, "q_{min}", f_μ; see Kaiser 2021, for details). However, $M_{\mathrm{grav,NS}}$ does show a dependence on the uncertainty, mainly due

https://doi.org/10.1017/S1743921322003349 Published online by Cambridge University Press

to the amount of chemical mixing occurring during the stellar evolution. Second, the non-magnetic models fail to predict the observed rotation rate of neutron stars because of missing angular momentum transport. Third, the two magnetic dynamos predict spin periods that are in the range of observations. However, the estimate of the models with the TS dynamo only covers the very fast rotating neutron stars, whereas the prediction by the models with the FTS dynamo agrees with the slower rotating neutron stars in the sample. None of the models manages to predict the full range of natal neutron star spin periods. Therefore, while the Tayler-Spruit dynamo does not transport enough angular momentum, the FTS version probably slows down the rotation cores too much. Salmon et al. (2022) show, using asteroseismic inference of the internal rotation of the β Cephei star HD 129929, that the FTS dynamo is definitely too strong for this star.

5. Discussion and Conclusion

We briefly investigated the evolution of the structure and rotation in massive stars and the impact of rotational and magnetic instabilities on the evolution of rotation. Importantly, magnetic instabilities bring the predicted spin of neutron stars much closer to the observed ones with the Tayler-Spruit dynamo reaching the fast end of observations and the Fuller-modified Tayler-Spruit dynamo reaching the slow end. Note, however that the comparisons above assume that the angular momentum content of the core at the time of the pre-collapse is the same as the one that will be locked into the neutron star, an hypothesis that may not be always correct. Furthermore, there are still major uncertainties concerning the theories used to describe rotation and magnetic fields in stars and their implementation. In particular, one has to be careful when comparing the predictions of different codes since the implementation of physical processes vary between codes. There are fortunately many other constraints from observations of stars in different mass ranges and evolutionary phases that are and will be able to constrain these processes and disentangle uncertainties. Examples include the key role of rotation and magnetic instabilities in the context of the solar modelling problem (Eggenberger et al. 2022), asteroseismology (see contributions by Burssens and Bowman in these proceedings; e.g. Pamyatnykh et al. 2004; Deheuvels et al. 2014; Aerts et al. 2019; Claret & Torres 2018; Pedersen et al. 2021; Salmon et al. 2022), the luminosity-mass plane (Higgins & Vink 2019), comparison of models to observations of low-mass stars and white dwarfs (Cantiello et al. 2014; Spada et al. 2016; Fuller & Ma 2019; Eggenberger et al. 2019a,b; den Hartogh et al. 2019, 2020). In addition multi-D simulations (e.g. Edelmann et al. 2017; Gagnier et al. 2019b; Varma & Müller 2021; Yoshida et al. 2021; Petitdemange et al. 2022) of stellar interiors will also help guide and constrain theories used in 1D models.

Acknowledgements

RH acknowledges support from the World Premier International Research Centre Initiative (WPI Initiative), MEXT, Japan and the IReNA AccelNet Network of Networks (National Science Foundation, Grant No. OISE-1927130). GM, SE, PE, CG acknowledge funding from the European Research Council (ERC) under the European Union's Horizon 2020 research and innovation program (Grant No. 833925). This article is based upon work from the ChETEC COST Action (CA16117) and the European Union's Horizon 2020 research and innovation programme (ChETEC-INFRA, Grant No. 101008324).

References

Aerts C., Mathis S., Rogers T. M., 2019, ARA&A, 57, 35
Braithwaite J., Spruit H. C., 2004, Nature, 431, 819
Caleo A., Balbus S. A., Tognelli E., 2016, MNRAS, 460, 338

Cantiello M., Mankovich C., Bildsten L., Christensen-Dalsgaard J., Paxton B., 2014, ApJ, 788, 93
Chieffi A., Limongi M., 2013, ApJ, 764, 21
Claret A., Torres G., 2018, ApJ, 859, 100
Cristini A., Meakin C., Hirschi R., Arnett D., Georgy C., Viallet M., Walkington I., 2017, MNRAS, 471, 279
Deheuvels S., et al., 2014, A&A, 564, A27
Edelmann P. V. F., Röpke F. K., Hirschi R., Georgy C., Jones S., 2017, A&A, 604, A25
Edelmann P. V. F., Ratnasingam R. P., Pedersen M. G., Bowman D. M., Prat V., Rogers T. M., 2019, ApJ, 876, 4
Eggenberger P., Meynet G., Maeder A., Hirschi R., Charbonnel C., Talon S., Ekström S., 2008, AP&SS, 316, 43
Eggenberger P., et al., 2019a, A&A, 621, A66
Eggenberger P., den Hartogh J. W., Buldgen G., Meynet G., Salmon S. J. A. J., Deheuvels S., 2019b, A&A, 631, L6
Eggenberger P., Buldgen G., Salmon S. J. A. J., Noels A., Grevesse N., Asplund M., 2022, Nature Astronomy, 6, 788
Ekström S., et al., 2012, A&A, 537, A146
Faucher-Giguère C.-A., Kaspi V. M., 2006, ApJ, 643, 332
Frischknecht U., Hirschi R., Meynet G., Ekström S., Georgy C., Rauscher T., Winteler C., Thielemann F. K., 2010, A&A, 522, A39
Fuller J., Ma L., 2019, ApJL, 881, L1
Fuller J., Piro A. L., Jermyn A. S., 2019, MNRAS, 485, 3661
Gagnier D., Rieutord M., Charbonnel C., Putigny B., Espinosa Lara F., 2019a, A&A, 625, A88
Gagnier D., Rieutord M., Charbonnel C., Putigny B., Espinosa Lara F., 2019b, A&A, 625, A89
Gotthelf E. V., Halpern J. P., Alford J., 2013, ApJ, 765, 58
Griffiths A., Meynet G., Eggenberger P., Moyano F., Aloy M. A., 2022, arXiv e-prints, p. arXiv:2204.00016
Heger A., Langer N., Woosley S. E., 2000, ApJ, 528, 368
Heger A., Woosley S. E., Spruit H. C., 2005, ApJ, 626, 350
Higgins E. R., Vink J. S., 2019, A&A, 622, A50
Hirschi R., Maeder A., 2010, A&A, 519, A16
Hirschi R., Meynet G., Maeder A., 2004, A&A, 425, 649
Hirschi R., Meynet G., Maeder A., 2005, A&A, 443, 581
Kaiser E., 2021, Ph.D. Thesis, Keele University
Kaspi V. M., Helfand D. J., 2002, in Slane P. O., Gaensler B. M., eds, Astronomical Society of the Pacific Conference Series Vol. 271, Neutron Stars in Supernova Remnants. p. 3 (arXiv:astro-ph/0201183)
Langer N., 1998, A&A, 329, 551
Ma L., Fuller J., 2019, MNRAS, 488, 4338
Maeder A., 1997, A&A, 321, 134
Maeder A., 2009, Physics, Formation and Evolution of Rotating Stars. Springer, doi:10.1007/978-3-540-76949-1
Maeder A., Meynet G., 2000, A&A, 361, 159
Maeder A., Meynet G., 2005, A&A, 440, 1041
Maeder A., Zahn J.-P., 1998, A&A, 334, 1000
Marshall F. E., Gotthelf E. V., Zhang W., Middleditch J., Wang Q. D., 1998, ApJL, 499, L179
Meynet G., Maeder A., 1997, A&A, 321, 465
Meynet G., Maeder A., 2002, A&A, 390, 561
Muslimov A., Page D., 1996, ApJ, 458, 347
Ogilvie G. I., 2014, ARA&A, 52, 171
Pamyatnykh A. A., Handler G., Dziembowski W. A., 2004, MNRAS, 350, 1022
Paxton B., Bildsten L., Dotter A., Herwig F., Lesaffre P., Timmes F., 2011, ApJS, 192, 3
Paxton B., et al., 2013, ApJS, 208, 4

Paxton B., et al., 2015, ApJS, 220, 15
Paxton B., et al., 2018, ApJS, 234, 34
Pedersen M. G., et al., 2021, Nature Astronomy, 5, 715
Petitdemange L., Marcotte F., Gissinger C., 2022, arXiv e-prints, p. arXiv:2206.13819
Petrovic J., Langer N., Yoon S. C., Heger A., 2005, A&A, 435, 247
Popov S. B., Turolla R., 2012, AP&SS, 341, 457
Popov S. B., Pons J. A., Miralles J. A., Boldin P. A., Posselt B., 2010, MNRAS, 401, 2675
Potter A. T., Tout C. A., Eldridge J. J., 2012a, MNRAS, 419, 748
Potter A. T., Chitre S. M., Tout C. A., 2012b, MNRAS, 424, 2358
Salmon S. J. A. J., Moyano F. D., Eggenberger P., Haemmerlé L., Buldgen G., 2022, A&A, 664, L1
Spada F., Gellert M., Arlt R., Deheuvels S., 2016, A&A, 589, A23
Spruit H. C., 2002, A&A, 381, 923
Talon S., Charbonnel C., 2005, A&A, 440, 981
Talon S., Zahn J. P., 1997, A&A, 317, 749
Tayler R. J., 1973, MNRAS, 161, 365
Varma V., Müller B., 2021, MNRAS, 504, 636
Wheeler J. C., Kagan D., Chatzopoulos E., 2015, ApJ, 799, 85
Yoshida T., Takiwaki T., Aguilera-Dena D. R., Kotake K., Takahashi K., Nakamura K., Umeda H., Langer N., 2021, Monthly Notices of the Royal Astronomical Society: Letters, 506, L20
Zahn J. P., 1974, in Ledoux P., Noels A., Rodgers A. W., eds, IAU Symposium Vol. 59, Stellar Instability and Evolution. p. 185
Zahn J. P., 1977, A&A, 57, 383
Zahn J.-P., 1992, A&A, 265, 115
den Hartogh J. W., Eggenberger P., Hirschi R., 2019, A&A, 622, A187
den Hartogh J. W., Eggenberger P., Deheuvels S., 2020, A&A, 634, L16

Discussion

Comment: 1D theoretical models for meridional circulation cells use one spherical harmonic. Recent 2D simulations show a different picture.

Answer: Good point. The theory described above is the one used in current stellar models. Multi-D simulations like those of Gagnier et al. (2019b), however, will provide key guidance for future theoretical developments.

Question: What about angular momentum transport in convective region?

Answer: As written above, stellar evolution codes assume constant Ω in convective zones. Potter et al. (2012a) investigated the impact of assuming uniform specific angular momentum in convective zones but more multi-D studies similar to those for the Sun would be welcome to better understand the distribution of angular momentum in convective regions in massive stars.

Question: What mass loss rates are being used for rotating models?

Answer: A modification factor is generally applied to mass loss rate prescriptions to take into account the effects of rotation (see Langer 1998; Maeder & Meynet 2000; Gagnier et al. 2019a, for details and discussions).

https://doi.org/10.1017/S1743921322003349 Published online by Cambridge University Press